LIGHT FRONT SOLUTION TO PROBLEMS OF CONVENTIONAL APPROACH TO DEEP INELASTIC ELECTRON-DEUTERON SCATTERING

By St. Głazek

Institute of Theoretical Physics, Warsaw University*

(Received April 15, 1986)

We present a model light front calculation of the inelastic electron-deuteron scattering within the conventional two nucleon approximation. The results lead to the clear interpretation of the convolution formula expressing structure functions of the deuteron by structure functions of nucleons. Several ambiguities of this formula, including the West-β correction and the Bodek ambiguity, are resolved. We use a simple quark model for the nucleon structure, guided by the counting rules. In extracting the neutron structure from the deuteron and the proton data we find that the dynamical off-shell effects in the nucleon structure functions are larger than the properly calculated smearing corrections.

PACS numbers: 13.60.Hb, 14.20.Dh

1. Introduction

In this paper we present a systematic analysis in light front dynamics of the inelastic electron-deuteron scattering within a conventional approach. The conventional assumption is that the deuteron is a loosely bound state of a proton and a neutron. One neglects other Fock components like e.g. sectors containing mesons, resonances, or hidden colour states of quarks at short distances. In fact, the deuteron would be unbound were it not for these other components but the deuteron binding energy [1] $\varepsilon = 2.224579(9)$ MeV is so small that one hopes to still have a good description neglecting them. Their contribution to the deep inelastic deuteron structure is not considered in this paper which is devoted to specific problems of the conventional approach itself.

According to the two nucleon approximation in a high energy electron-deuteron collision a single photon transfers a momentum q from the electron to one of the nucleons, ($-q^2 = Q^2 \sim$ from a few to hundreds of GeV^2). The photon is absorbed by the struck nucleon leaving the spectator nucleon untouched. For example interference effects among

* Address: Instytut Fizyki Teoretycznej, Uniwersytet Warszawski, Hoża 69, 00-681 Warszawa, Poland.

quarks of the struck and the spectator nucleons are consequently neglected according to the two nucleon approximation. The spectator nucleon is directly counted in the final state. The inclusive cross section for electrons can be expressed by the deuteron inelastic tensor $W_D^{\mu\nu}$. The conventional two nucleon incoherent approximation amounts to writing a formula

$$W_D^{\mu\nu}(D, q) = \sum_N \int d^3p \varrho(p) W_N^{\mu\nu}(p, q), \tag{1}$$

which is supposed to follow from a diagram of Fig. 1. However, without detailed model calculations of such diagram Eq. (1) contains factors of ambiguous meaning.

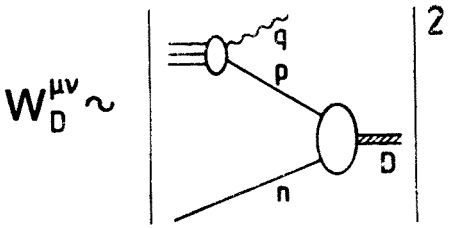

Fig. 1. The incoherent impulse approximation to the deep inelastic deuteron structure. Our convention is to denote the active nucleon by p and the spectator one by n. We read the diagram from the right hand side to the left hand side

The ambiguities are expected to be small, of the order of a few percent, but the desired accuracy is also high. For example, the extraction of the neutron structure doubles the error, and the d/u ratio in nucleons, being one of the most important properties of nucleons, contains an even more magnified error. Note also, that the so called EMC effect, i.e. the striking difference between the structure functions of deuteron and the structure functions of heavier nuclei, is of the order of 10%. The EMC effect raised a lot of speculations about the building blocks of nuclei, if they are really protons and neutrons as free ones, or if there are other important constituents in nuclei. Therefore it is essential to remove ambiguities which already show up in the simplest approximation like that of Eq. (1), in preparation to the more complicated questions mentioned above. This paper shows how the light front dynamics [2] answers some specific questions concerning Eq. (1) within the two nucleon approximation. Considering the diagram of Fig. 1 with the spectator nucleon directly counted in the final state we face the following problems:

1) Is the spin averaged deuteron structure $W_D^{\mu\nu}$ factorizing into a scalar density like $\varrho(p)$, and the spin averaged off-shell nucleon structure $W_N^{\mu\nu}$?

2) What is the physical interpretation of the function $\varrho(p)$ and how is it related, if at all, to the Schrödinger wave function $\Psi(\bar{p})$ of deuteron?

3) How is the off-shell nucleon structure tensor $W_N^{\mu\nu}(p, q)$ related to the free nucleon structure tensor?

4) Is it possible to find a connection among the free nucleon structure functions and the off-shell structure functions of virtual nucleons from Eq. (1) such that the longitudinal deuteron cross section vanishes in the limit $q^2 \to 0$, without ad hoc corrections?

5) Does the formula (1) lead to the parton model expectations in the Bjorken limit?

6) How to extract the neutron structure functions from the proton and the deuteron data?

There exist many attempts to bypass these problems in the literature [14, 18–22]. For completeness we shortly discuss these approaches in Section 6. Here we only mention that we do not completely agree with any one of them. Only the light front approach admits Eq. (1) in the two nucleon approximation of Fig. 1 without artificial corrections invented to remove unwanted features. Moreover, the light front approach is well prepared for including other sectors of hadronic components without introducing new principal difficulties on the phenomenological level [2, 3]. The urgent need for such a consistent approach originates also from the fact that problems of the same kind are met in extracting quark properties from hadronic structure.

The remainder of the paper is organized as follows.

In Sec. 2 we consider the kinematics of the electron-deuteron scattering and describe the basic dynamical reasons why the light front approach is so much favoured to other schemes.

Section 3 outlines the derivation of the deuteron wave function, giving us the density $\varrho(p)$ in Eq. (1). Before treating the deuteron structure $W_D^{\mu\nu}$ we first make a simple model of the nucleon, in terms of an active quark a, and a passive core c, guided by counting rules.

Section 4 contains detailed calculations of the nucleon structure functions. They are expressed by the virtual Compton scattering amplitude on the active quark, smeared with the nucleon-quark-core wave function. We do not consider perturbative scaling violations and carry out calculations on the level of a simple parton-like picture.

The main Section 5 shows how the deuteron structure functions can be expressed by the off-shell continued structure functions of the nucleons in the two nucleon approximation of Fig. 10. The smearing of the virtual Compton scattering amplitude on the active quark is different in the nucleon belonging to the deuteron than in the free nucleon. We call this effect the dynamical effect, and discuss its size, in the ratio to the properly calculated effects of the Fermi motion, and its influence on the extracted neutron structure function $F_{2N}(x)$.

In Section 6 we briefly discuss other methods used in the analysis of electron-deuteron scattering.

Finally, in Sec. 7 we summarize our basic results.

2. Basic kinematics and dynamics

This Section contains rudimentary facts simplifying the light front approach to the deuteron structure, in comparison to other approaches, [2, 3]. We describe the absorption of a virtual photon by a target. The photon carries spatial momentum transfer q, $(Q^2 = -q^2 > 0)$, emitted by the electron observed in a laboratory. The target has a four-momentum D, $M^2 = D^2$, being at rest in the laboratory. Two momenta q and D distinguish a class of zero-vectors η defining light fronts $\eta x = x^+ = 0$. Once we use one

of such light fronts to develop the light front dynamics of the photon absorption by the deuteron we can approximate the deuteron by its two nucleon Fock sector, and the problems listed in Sec. 1 are altogether resolved.

The class of zero-vectors is given by the following equation

$$\eta = \frac{2xD+q}{2xM+\nu} + \sqrt{\frac{2xM}{2xM+\nu}}\,\zeta, \tag{2}$$

where

$$x = \frac{Q^2}{2Dq}, \quad \nu = \frac{Dq}{M}, \tag{3}$$

and the otherwise arbitrary four-vector ζ satisfies conditions

$$\zeta D = \zeta q = 0, \quad \zeta^2 = -1. \tag{4}$$

The same definition of η can be used in elastic, quasi-elastic, or inelastic electron--deuteron scattering, as well.

To explain the meaning of η we go to the rest frame of the deuteron, i.e. the laboratory frame, where we have

$$\begin{aligned} D &= (M, \vec{O}), \\ q &= (\nu, \vec{q}), \\ \zeta &= (O, \vec{\zeta}), \quad \vec{\zeta} \perp \vec{q}, \end{aligned} \tag{5}$$

so

$$\eta^0 = 1, \vec{\eta} = \sqrt{\frac{2xM}{2xM+\nu}}\,\vec{\zeta} + \frac{\vec{q}}{2xM+\nu}. \tag{6}$$

Then, rotating the spatial coordinate axes in such a manner that

$$\vec{e}_z = -\vec{\eta}, \tag{7}$$

we get a configuration depicted in Fig. 2. The freedom left to the vector $\vec{\zeta}$ in Eq. (4) means that the z axis has to lie on a surface of the cone defined by the vector $\vec{q}$ and an angle $\alpha = \operatorname{arctg} \frac{Q}{\nu}$. This freedom amounts to a choice of the azimuthal angle φ fixing the direction of $\vec{q}^{\perp}$ in the transverse plane. In the deep inelastic limit when Q and ν tend to infinity, while $\frac{Q^2}{\nu}$ is kept constant, the angle α tends to zero. Therefore the z axis tends to the vector $\vec{q}$ direction, but, although $\alpha \to 0$, we always have $-q^2 = (\vec{q}^{\perp})^2 = Q^2 \to \infty$. In other words the properly chosen vector $\vec{e}_z$ points along the vector $-\vec{q}$ in the laboratory, in the sense that the angle α between these vectors tends to zero like $\frac{\text{const}}{Q}$. Nevertheless, the

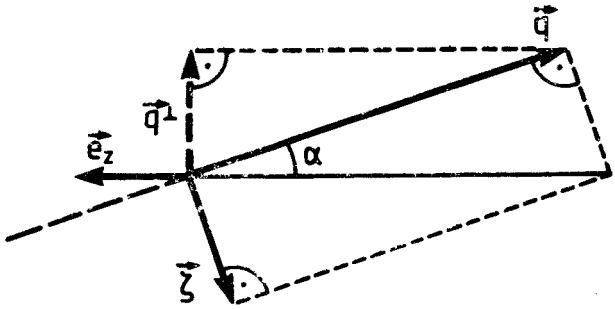

Fig. 2. Kinematical configuration in the laboratory frame, with the z axis chosen according to Eqs. (2) and (7). $\mathrm{tg}\,\alpha = \frac{Q}{\nu}$, and α goes to zero in the deep inelastic limit, but $q^2 = Q^2$ is always equal to $q^2 = -\vec{q}^{\perp 2}$, because $q^+ = \eta q = 0$

transverse component $\vec{q}^{\perp} = \vec{q} - (\vec{e}_z\vec{q})\vec{e}_z$ tends simultaneously to infinity, $|\vec{q}^{\perp}| = Q$, and the relation $-q^2 = Q^2 = (\vec{q}^{\perp})^2$ is always satisfied. It is this subtle deviation of the z-axis from the vector $\vec{q}$ which is necessary to develop the light front dynamics curing problems listed in Sec. 1.

Now we explain how the above choice of kinematical configuration is motivated by the principles of the light front dynamics. The formula (2) for the light front vector η follows from the conditions:

$$\eta^2 = 0, \tag{8a}$$

$$\eta q = 0, \tag{8b}$$

$$\eta D = M. \tag{8c}$$

We use the null-vector η (condition (8a)) to develop the light front dynamics [2, 3]. The condition (8b) gives

$$0 = \eta q = \tfrac{1}{2}\eta^+ q^- + \tfrac{1}{2}\eta^- q^+ - \eta^\perp q^\perp = q^+ = q^0 + q^3 \tag{9}$$

where we used the normalization condition (8c), and Eq. (7). In the light front dynamics the + component of momentum is conserved, and is always positive. Therefore, the limiting value $q^+ = \eta q \to 0$ eliminates contributions from pair creations by the photon. Using the + component of the electromagnetic currents (so called "good currents" [7]) we eliminate the seagull contributions. Finally, our relativistic expressions for form factors look like the nonrelativistic integrals with wave functions [4]. With the only exception, that the wave functions are now the correctly boosted light front wave functions, with the properly adjusted light front direction. The deuteron wave function is described in Sec. 3, where we also show the unique resemblance between the light front two nucleon Fock component of the deuteron and the nonrelativistic Schrödinger wave function for the two nucleon bound state.

The light front dynamics is invariant under three independent Lorentz boosts. Thanks to this advantage one can take into account relativistic effects of the motion of nucleons inside the deuteron. It is sufficient to know the structure of a nucleon at rest.

Thus, in order to derive the formula (1), we are led to the light front form of dynamics, with the particular light front definition following from experimental conditions, and the conventional approximations, which we are forced to make.

3. The deuteron wave function

Our calculation of the deuteron structure tensor $W_D^{\mu\nu}$ is guided by the old-fashioned light front perturbation theory [2, 3]. In this Section we show how the relevant deuteron vertex, used in the calculation, can be related to the known deuteron wave function (see also Sec. 6 for the discussion of the ambiguities encountered in other approaches). It is sufficient to consider the deuteron at rest, because the light front dynamics is invariant under three independent boosts.

The state equation in the light front dynamics is written as

$$P^-|M\rangle = M|M\rangle \tag{10}$$

and it corresponds to the equation $P^0|M\rangle = M|M\rangle$ in the time-instant form of dynamics. Elimination of all other Fock components leads to the effective two nucleon equation, called the Weinberg equation [5], with the effective interaction V_{eff}, (see Fig 3). We introduce the relative momentum of nucleons

$$k = \tfrac{1}{2}(p-n), \tag{11}$$

which in the center of mass of the nucleons takes the form

$$k = (0, \vec{k}), \quad k^2 = -\vec{k}^2. \tag{12}$$

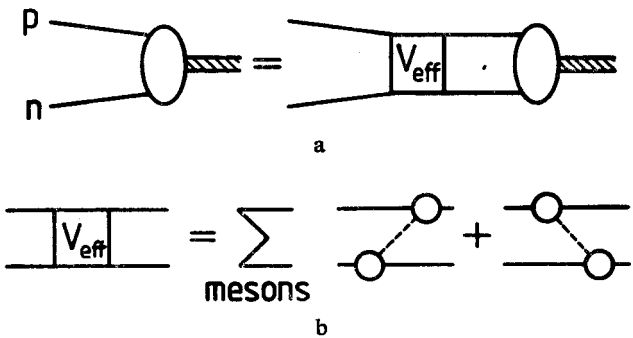

Fig. 3. a) The effective Weinberg equation for the two nucleon component of the deuteron state. b) An example of the effective nucleon-nucleon interaction in the approximation of one meson exchange. The blobs in vertices denote form factors. Only the two nucleon component of the deuteron is considered in the conventional approach

Changing variables $(k^+, k^\perp)$ to $(\vec{k}) = (k^3, \vec{k}^\perp)$ we get

$$\int_{\frac{-M}{2}}^{\frac{M}{2}} dk^+ \frac{1}{p^+ n^+} d^2k^\perp = \frac{4}{M} \int_{-\infty}^{\infty} dk^3 \frac{1}{M_k} d^2k^\perp, \tag{13}$$

where $M_k = 2\sqrt{m^2+\vec{k}^2}$ and m is the nucleon mass. The Weinberg equation reads

$$\phi(\vec{k}) = G_0 \sum_{\substack{\text{spins} \\ \text{isospins}}} \int \frac{d^3k'}{2(2\pi)^3 M_{k'}} V_{\text{eff}}(\vec{k}, \vec{k}'; M)\phi(\vec{k}'). \tag{14}$$

The propagator G_0 is equal to

$$-G_0 = \frac{4}{M(p^- + n^- - M)} = (m\varepsilon + \vec{k}^2)^{-1} \tag{15}$$

where ε is the deuteron binding energy.

The propagator in the fully relativistic Weinberg equation is exactly the same as in the nonrelativistic Schrödinger equation. All relativistic features are built into the effective potential, and into the integration measure $d^3k'/M_{k'}$. Therefore the Weinberg wave function approaches the nonrelativistic wave function, evaluated in the appropriate potential.

To decide whether the Weinberg and the Schrödinger wave functions differ by a factor like $(M_k)^{1/2}$ (see Sec. 6) we consider an extreme case of the effective potential following from an exchange of a very heavy meson of mass $\delta \gg m$. Then for momenta $|\vec{k}|, |\vec{k}'| \ll \delta$ the kernel V_{W}^{δ} in the Weinberg equation, and the appropriate potential V_{NR}^{δ} in the Schrödinger equation (the limit $\left|\frac{\vec{k}}{m}\right| \to 0$ of V_{W}^{δ}) are independent of the momenta $\vec{k}$ and $\vec{k}'$. Therefore, for momenta $|\vec{k}| \sim m \ll \delta$, in the integral equations

$$\phi(\vec{k}) = \frac{1}{m\varepsilon + \vec{k}^2} \int \frac{d^3k'}{(2\pi)^3 2M_{k'}} V_{\text{W}}^{\delta}(\vec{k}, \vec{k}'; M)\phi(\vec{k}')$$

$$\phi_{\text{NR}}(\vec{k}_{\text{NR}}) = \frac{1}{m\varepsilon + \vec{k}_{\text{NR}}^2} \int \frac{d^3k'_{\text{NR}}}{(2\pi)^3 2M_{k'}} V_{\text{NR}}^{\delta}(\vec{k}_{\text{NR}}, \vec{k}'_{\text{NR}}) \cdot \phi_{\text{NR}}(\vec{k}'_{\text{NR}}) \tag{16}$$

we can neglect the k-dependence of both V_{W}^{δ} and V_{NR}^{δ}. It is transparent that the Weinberg wave function $\phi(\vec{k})$ differs from the Schrödinger wave function $\phi_{\text{NR}}(\vec{k}_{\text{NR}} = \vec{k})$ only by a constant factor, independent of $\vec{k}$, even for $|\vec{k}| \sim m$. The well-known form $r^{-1} \exp(-\sqrt{m\varepsilon}r)$ of the deuteron wave function, outside the range of a potential, being the Fourier transform of $(m\varepsilon + \vec{k}^2)^{-1}$, has its universal relativistic counterpart in the light front wave function, no matter how small the range of the potential is.

There is no ambiguity in the light front dynamics how to identify the relativistic wave function with the nonrelativistic one. The ambiguity is resolved by the Weinberg equation.

The widely discussed factor $\sqrt{m^2+\vec{k}^2}$ (see Sec. 6) is not present in the wave function. Nevertheless it is present in the integration measure in relativistic formulae.

The deuteron has spin one. In the light front dynamics the angular momentum operator depends on the interaction. However, the effective potential V_{eff} is known only approximately and the angular momentum problem is not solved exactly. This is the weakest point of the light front approach. It can be bypassed using a particular basis of spinors [6], and classifying the angular momentum eigenstates according to the rules given by Leutwyler and Stern [7], with the particular spin labels identified with the nonrelativistic ones. This is possible thanks to the unique property of the light front spinors that they do not undergo the Wigner rotations under three independent boosts, under which the light front dynamics is invariant [6]. Therefore the spin labels, carried by these spinors, can be identified with the nonrelativistic Pauli spin indices, which are not influenced by the motion of a fermion.

The deuteron vertex function is given by the formula

$$g_{\text{D}} = D^+(p^- + n^- - D^-)2(2\pi)^3\delta^{+,\perp}(p+n-D)\cdot\Phi\cdot i\tau_2. \tag{17}$$

τ_2 is the isospin matrix. The wave function Φ contains appropriate matrices giving

$$(\bar{\tilde{u}}_{s_{\text{p}}})_\alpha\,(\bar{\tilde{u}}_{s_{\text{n}}})_\beta\Phi_{\alpha\beta} = \chi^+_{s_{\text{p}}}\left[\phi_0(\vec{k})\cdot\vec{\sigma}\vec{s} + \frac{\phi_2(\vec{k})}{\sqrt{2}}\left(3\,\frac{\vec{k}\vec{\sigma}\cdot\vec{k}\vec{s}}{\vec{k}^2} - \vec{\sigma}\vec{s}\right)\right] i\sigma_2\chi_{s_{\text{n}}}, \tag{18}$$

where the spin indices s_{p}, s_{n} refer to the special spinor representation $\tilde{u}$ from Ref. [6] and $\vec{s}$ is the deuteron spin vector in its rest frame [8]. If the outgoing deuteron forms the last vertex of a diagram one omits the factor $2(2\pi)^3\delta^{+,\perp}(p+n-D)$ in g^*_{D}.

The normalization of the deuteron vertex follows from the deuteron current j^+_{D} at zero momentum transfer, calculated according to Fig. 4. One uses the vertex factorization property of the light front rules [9] and, within the two nucleon approximation, one can write

$$\int \frac{d^3k}{(2\pi)^3}\,\frac{m}{\sqrt{m^2+\vec{k}^2}}\,(\phi_0^2+\phi_2^2) = 1 \tag{19}$$

if the proton charge is normalized to unity. The proton is in a virtual state, and its quark content, i.e. its quark Fock space expansion, is continued off-shell in the minus component

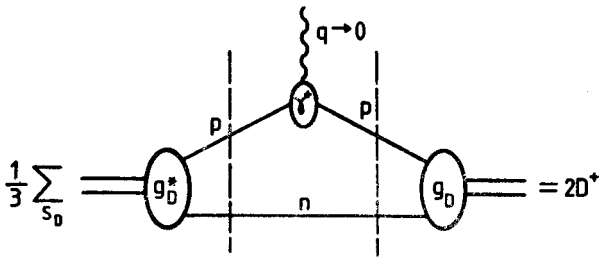

Fig. 4. The deuteron current j^+_{D} at $q \to 0$ normalizes the deuteron vertex function g_{D}. Two broken lines depict the intermediate states. Their denominators cancel the denominators factored out in Eq. (17), after summing the orderings of the external electromagnetic vertex

of the total momentum P^-. Therefore, the normalization of its charge, as well as for the neutron, provides a nontrivial sum rule for the off-shell continued structure functions, which we use in Sec. 5.

4. Simplified model of nucleons

We construct a model of nucleons assuming that their structure can be approximated by an active valence quark a, and a passive core c [3, 10, 11]. The core c represents all states accompanying the photon absorption by the active quark, Fig. 5. The quark-core model for the nucleons is imbedded in the deuteron in the next Section, where we calculate the deuteron deep inelastic structure.

Our simplified model of nucleons describes some basic properties of nucleons, relevant to the analysis of the deuteron structure function, because:

1) It respects the light front spin conservation in the hard elastic scattering [3].
2) It gives the asymptotic behaviour of elastic nucleon form factor $F_1(Q^2) \sim (Q^2)^{-2}$
3) It satisfies the condition that in the deep inelastic scattering for $x_{Bj} \to 1$ the active quark carries the spin of the nucleon.
4) It gives the structure function $F_2 = xF_1$ behaving for $x \to 1$ as $(1-x)^3$
5) It possesses the unique off-shell continuation in the deuteron, according to the light front rules.
6) It fulfills the charge sum rule.
7) It fits thé experimental data for $F_{2p}(x)$ for $x \gtrsim 0.3$ (sea quarks are not explicitly counted).

To keep control of the off-shell behaviour of our nucleons in the deuteron we treat the momentum-dependence of the nucleon-quark-core vertex as in the tree diagram in Fig. 6

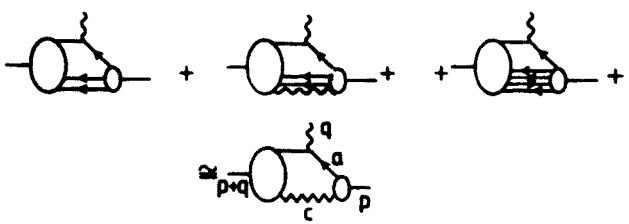

Fig 5. Matrix element of the electromagnetic current between the initial nucleon of momentum p, and the final state of momentum $p+q$, approximated by the quark-core model

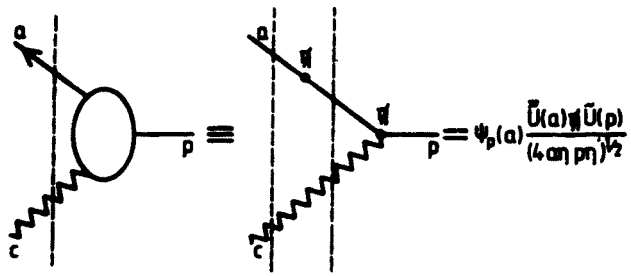

Fig. 6. The momentum-dependence of the nucleon-quark-core vertex, denoted by $\psi_p(a)$. It is assumed to be given by the tree diagram. The vertex matrix $\not{n} = \gamma^+$ plays an essential role in our derivation of Eq. (1)

The additional vertex, marked by a dot on the quark line, resembles the valon description of the quark distribution in nucleons [13]. The two intermediate states, contributing two denominators in perturbation theory, are necessary to reproduce results of counting rules [3]. We use the notation, which is useful in the later application to the deuteron, and write

$$\psi_p(a) = N(p)\,[a^+(p^- - a^- - c^-)]^{-2} = N(p)\,[(p-c)^2 - m_a^2]^{-2}. \tag{20}$$

In deuteron the minus component p^- is replaced by $D^- - n^-$, so we have

$$p^- = \frac{p^{\perp 2} + m^2}{p^+} \to \tilde{p}^- = D^- - n^- = \frac{p^{\perp 2} + (D-n)^2}{p^+},$$

$$\tilde{p}^{+,\perp} = p^{+,\perp} \tag{21}$$

and the normalization constant $N(p) = N(p^2)$ changes to $N(\tilde{p}^2)$, which is fixed by the charge sum rule (24).

The nucleon-quark-core vertex is constructed to contain $\not{\eta} = \gamma^+$, to conserve the light front spin, and to make it possible to derive Eq. (1), as is explained later. The vertex η yields also the conserved elastic nucleon current j_p^ν.

According to Fig. 7 the elastic nucleon form factor, extracted from the + component of the nucleon current j_p^+, is given as follows

$$\gamma^+ F_1(Q^2) = \sum_i \int \frac{dc^+ d^2c^\perp}{2(2\pi)^3 c^+}\, \psi_{p'}^{i*}(a')\, \frac{1}{4p^+ a^+}\, \not{\eta}(\not{a}' + m_a) e_i \gamma^+ (\not{a} + m_a) \not{\eta} \psi_p^i(a). \tag{22}$$

We shall omit the sum over flavours and charges e_i in the following equations, neglecting differences between the up and down quarks distributions, which are interesting, but are not directly relevant to our present analysis. The nucleon vertex description, including the flavour-dependence, based on the QCD sum rules, and on the concept of an effective quark mass, combined with the perturbative QCD, is presented in the second of Refs. [4], and in Ref. [12]. Using an abbreviation

$$\frac{1}{2(2\pi)^3} \int_0^{p^+} \frac{dc^+}{c^+} \int_{-\infty}^{\infty} d^2c^\perp \equiv \int [dc], \quad a^{+,\perp} = p^{+,\perp} - c^{+,\perp} \tag{23}$$

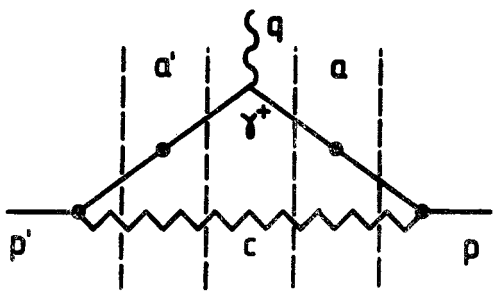

Fig. 7. The elastic nucleon current j_p^+ ($q^+ = 0$)

the normalization condition at $Q^2 = 0$ (which is the charge sum rule) reads

$$F_{1p}(0) = \int [dc] \frac{a^+}{p^+} |\psi_p(a)|^2 = 1. \tag{24}$$

The inelastic electron-deuteron scattering cross section is

$$\frac{d\sigma_p}{d\Omega_e dE'} = \frac{\alpha^2}{Q^4} \frac{E'}{E} \left(\frac{1}{2} \sum_{s_e s_{e'}} j^{\mu *} j^{\nu}_e \right) \cdot W^{\mu\nu}_p, \tag{25}$$

where the nucleon structure tensor $W^{\mu\nu}_p$ beyond the resonance region can be expressed as (see Fig. 8)

$$W^{\mu\nu}_p = \frac{1}{2} \sum_{s_p} \frac{1}{2m} \int \sum_{s_{a'}} [da'] [dc] (2\pi)^3 \delta^4(p+q-a'-c) \cdot j^{\mu *}_p \cdot j^{\nu}_p. \tag{26}$$

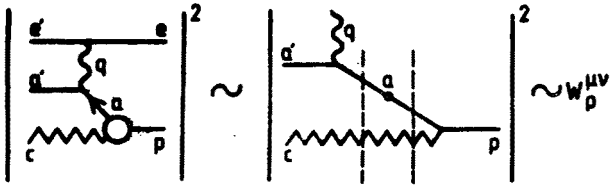

Fig. 8. The deep inelastic nucleon structure tensor $W^{\mu\nu}_p$

The nucleon current j^{ν}_p is

$$j^{\nu}_p = \bar{\tilde{u}}(a') \gamma^{\nu} (\not{a} + m_a) \not{\eta} \tilde{u}(p) (4p^+ a^+)^{-1/2} \psi_p(a) \tag{27}$$

Note that neither a^-, nor p^-, nor the masses occurring in the sums over spins enter in Eq. (27). This feature enables us to derive Eq. (1) in the next Section, and it follows from the property of the light front vector η that $\eta^2 = \eta^2 = 0$. The nucleon tensor $W^{\mu\nu}_p$ calculated in Appendix from Eq. (26) for $\mu, \nu = +, \perp$ has the form

$$W^{\mu\nu}_p = -W_1 \left(g^{\mu\nu} - \frac{q^\mu q^\nu}{q^2} \right) + \frac{W_2}{m^2} \left(p^\mu - \frac{pq}{q^2} q^\mu \right) \left(p^\nu - \frac{pq}{q^2} q^\nu \right), \tag{28a}$$

where the structure functions W_1 and W_2 are

$$W_{1p}(q^2, pq, p^2) = \frac{1}{2m} \int [dc] \frac{1}{a^+} \delta(p^- + q^- - a'^- - c^-) \tfrac{1}{2} |\psi_p(a)|^2 (-2q^2 + 8(a^\perp q)^2),$$

$$W_{2p}(q^2, pq, p^2) = \frac{m}{p^{+2}} \frac{1}{2m} \int [dc] \frac{1}{a^+} \delta(p^- + q^- - a'^- - c^-) \tfrac{1}{2} |\psi_p(a)|^2 8a^{+2}. \tag{28b}$$

In the Bjorken limit $q^- \to \infty$, $Q^2 \to \infty$, $Q^2/2pq = x_{Bj}$ fixed, the argument of the delta function simplifies to

$$\delta(p^- + q^- - a'^- - c^-) = \frac{a^{+2}}{Q^2}\,\delta\left(a^+ - \frac{Q^2}{2\nu}\right), \quad \frac{a^+}{p^+} = x = x_{Bj}, \tag{29}$$

and the structure functions become

$$F_1(p^2, x) = 2mW_1 = N(p^2)x^{-2}\left[\frac{m_a^2}{x} + \frac{m_c^2}{1-x} - p^2\right]^{-3},$$

$$F_2(p^2, x) = \nu W_2 = xF_1(p^2, x). \tag{30}$$

The normalization condition (24) results in the sum rule

$$\int_0^1 dx\,\frac{F_2(p^2, x)}{x} = 1. \tag{31}$$

For $x \to 1$ the structure function F_2 behaves as $(1-x)^3$ and Eq. (30) can reproduce the experimental data for $x \gtrsim 0.5$. For $x < 0.5$ the active quark does not have to carry the spin of a nucleon, and the vertex $\not{n}$ is not sufficient. In our phenomenological estimates of the dynamical effects in the deuteron we improve in Sec. 5 Eq. (30) for $x < 0.5$ by the substitution

$$x^{-1}\left[\frac{m_a^2}{x} + \frac{m_c^2}{1-x} - p^2\right]^{-3} \to x^{\alpha}\left[\mu^2 + \frac{m_c^2}{1-x} - p^2\right]^{-3}. \tag{32}$$

From the Regge behaviour of the parton-proton amplitude [11] it is expected that $\alpha \sim \frac{1}{2}$. The parameter μ^2, replacing the effective quark mass divided by x is of the order of the nucleon mass. Note that the phenomenological improvement Eq. (32) preserves the essential dependence on p^2, which goes over to $(D-n)^2$ in deuteron, as shown in the next Section. The resulting proton structure function F_2 is plotted in Fig. 9.

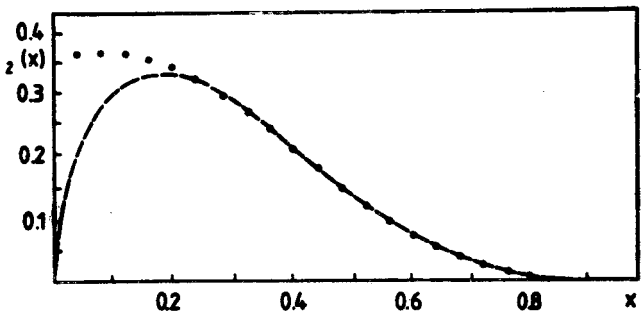

Fig. 9. The proton structure function $F_2(x)$, given by Eqs. (30), (31) and (32), for $m_c = 0.85$ GeV, $\mu = 0.9$ GeV, and $\alpha = 0.67$. The points represent the fit to the data at $Q^2 = 15$ GeV^2, from Ref. [14]

5. Nucleons in deuteron

A. Structure functions of the deuteron

The deuteron structure functions are calculated by imbedding the nucleon model of Sec. 4 into the deuteron inelastic current according to Fig. 10. Beyond the resonance region the deuteron inelastic tensor is given by (cf. Eqs. (26) and (27))

$$W_D^{\mu\nu} = \tfrac{1}{3} \sum_{s_D} \frac{1}{2M} \sum_{p=\text{proton}}^{\text{neutron}} \int [dn] \sum_{s_n} \int [da'] \sum_{s_{a'}} \int [dc]$$

$$\times (2\pi)^3 \delta^4(D+q-a'-c-n) \cdot j_D^{\mu *} \cdot j_D^{\nu}, \tag{33}$$

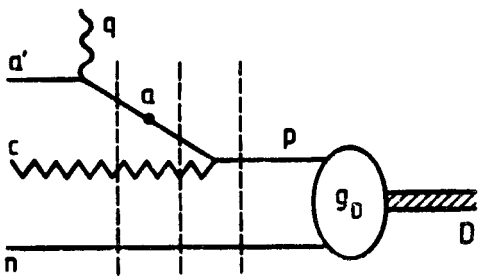

Fig. 10. The deuteron inelastic current expressed by the active quark current according to the nucleon model from Fig. 6. The deuteron vertex g_D is given by Eq. (17) in Sec. 3

where the deuteron current is

$$j_D^{\nu} = \sum_{s_p} \bar{\tilde{u}}(a')\gamma^{\nu}(\not{a}+m_a)\not{n}\tilde{u}(p)\,(4p^+a^+)^{-1/2}\psi_{\tilde{p}}(a)\,\frac{D^+}{a^+}\,\phi_{s_p s_n} \tag{34}$$

and the deuteron wave function $\phi_{s_p s_n}$ is expressed by the matrix Φ from Eq. (17). Both nucleons are described by their on-mass-shell spinors. The sum over their spins in the intermediate Fock state (off-shell in total P^-), averaged over the deuteron spin, factorizes into

$$(\phi_0^2+\phi_2^2)\,\tfrac{1}{2}\,(\not{p}+m). \tag{35}$$

Such factorization does not occur if one uses the Feynman rules with $(\not{\tilde{p}}+m)$ in the numerator of the active nucleon, and the deuteron vertex like e.g. $\not{S}C$ (see also discussion in Sec. 6). There one obtains not only terms like $(\not{\tilde{p}}+m)\cdot\varrho$ which could result in the off--shell continued structure functions times the scalar density ϱ, but also terms proportional to $(\tilde{p}^2-m^2)\cdot\Gamma$, which contain matrices Γ different from $(\not{\tilde{p}}+m)$, and do not lead to Eq. (1).

From Eq. (33) it follows that the deuteron structure tensor is

$$W_D^{\mu\nu} = \frac{1}{2M} \sum_{\substack{\text{neutron} \\ p = \text{proton}}} \int [dn] \left(\frac{D^+}{p^+} \right)^2 (\phi_0^2 + \phi_2^2) \cdot \tfrac{1}{2} \int [dc] \, (\psi_{\tilde{p}}(a))^2$$

$$\times \frac{1}{4p^+ a^+} \operatorname{Tr} [\not{n}(\not{l} + m_a)\gamma^\mu(\not{q}' + m_a)\gamma^\nu(\not{l} + m_a)\not{n}(\not{p} + m)] \frac{1}{a^+} \delta(\tilde{p}^- + q^- - a'^- - c^-), \tag{36}$$

where

$$\tilde{p} = D - n. \tag{37}$$

By comparison with Eq. (A.1) for the nucleon structure function (see Appendix) we get that Eq. (36) is selfcontradictory. Namely, the momentum-dependent nucleon vertex $\psi_{\tilde{p}}(a)$ is continued off-shell from p to $\tilde{p}$, while the spin trace in Eq. (36) contains the on-mass-shell momentum $\not{p}$, as the necessary condition for the factorization property in Eq. (35). Therefore, without the essential property of the light front vector η given by

$$\not{\eta}^2 = 0 \tag{38}$$

the factorization, and the off-shell continuation are contradictory.

The intermediate states in the x^+-ordered perturbation theory are off-shell in the P^- component of the total momentum. In other words, one continues off-shell in the total momentum along the light front vector η. This is the continuation $\psi_p(a) \to \psi_{\tilde{p}}(a)$. Nevertheless, the spin sum $(\not{p} + m)$ contains the on-mass-shell momentum p, and the nucleon mass m which are the same as for free nucleons and are not continued off-shell. These follow from the fact that there are no seagull diagrams for composite nucleons. Fortunately, the troublesome sum $(\not{p} + m)$ is sandwiched with nucleon vertices which we have chosen to contain $\not{\eta}$ conserving the light front spin. Hence

$$\not{n}(\not{p} + m)\not{n} = 2p^+ \not{n} \tag{39}$$

and the nucleon structure functions are uniquely continued off-shell from p to $\tilde{p}$, see Eq. (21). The same mechanism eliminates seagull contributions from the j^- current matrix elements [3]. Our model provides a selfconsistent example in which the deuteron structure tensor $W_D^{\mu\nu}$ calculated from the diagram of Fig. 10 is factorized according to Eq. (1).

Repeating the steps from the Appendix and changing variables n^+, $\vec{n}^\perp$ to $\vec{k}$ according to Eq. (13) we get the result

$$W_{1D} = \sum_{\substack{\text{neutron} \\ p = \text{proton}}} \int d^3k f(\vec{k}) \frac{m}{p^+} \left[W_{1p} + \frac{p^{\perp 2}}{2m^2} W_{2p} \right],$$

$$W_{2D} = \sum_{\substack{\text{neutron} \\ p = \text{proton}}} \int d^3k f(\vec{k}) \frac{m}{p^+} \left[\frac{p^{+2}}{m^2} W_{2p} \right]. \tag{40}$$

We discuss this result in the deuteron rest frame. The deuteron structure functions W_{1D} and W_{2D} depend on the variables q^2 and $Dq = 2Mv$.

The smearing function $f(\vec{k})$ is

$$f(\vec{k}) = \frac{1}{(2\pi)^3} \frac{m}{\sqrt{m^2+\vec{k}^2}} (\phi_0^2+\phi_2^2), \tag{41}$$

where $\phi_0(\vec{k})$ and $\phi_2(\vec{k})$ are the light front deuteron S and D wave functions, respectively, discussed in Sec. 3. They can be identified with the nonrelativistic wave functions, if the solution to the Weinberg equation, explaining the experimental results including the weight $(m^2+\vec{k}^2)^{-1}$, is not available. Nevertheless, the interpretation of $\varrho(p)$ in Eq. (1) is clear.

B. Identification of the virtual nucleon structure functions

The structure functions W_{1p} and W_{2p} in Eq. (40) are given by Eq. (28), with the replacement $p \to \tilde{p}$. We use Eq. (28) in the Bjorken limit in next Sections to discuss the dynamical off-shell effects. Here we consider the identification of the virtual nucleon structure functions independently of the particular model Eq. (28), but preserving the general properties of the light front scheme.

The structure functions W_{1p} and W_{2p} are functions of two momenta $\tilde{p}$ and q. The momentum transfer q carried by photon is defined by the external electron and it is the same both for the free and the bound nucleon. The momentum q is not modified in the identification of the virtual structure functions. Thresholds in the bound nucleon structure occur with the variations of the invariant mass $(D-n+q)^2 = (\tilde{p}+q)^2$. To preserve the threshold behaviour one has to treat the virtual structure functions as functions of the final mass $W^2 = (\tilde{p}+q)^2$. If $(\tilde{p}+q)^2 < m^2$, then the structure functions vanish. Once a model-independent description of the $\tilde{p}^2$-dependence of the virtual functions is not available one can try to identify the virtual structure functions with physical ones, according to the above rules, without separate variation of $\tilde{p}^2$. However, such a procedure in conventional approaches (see Sec. 6) violates the physical condition [10] that the deuteron longitudinal cross section should vanish in the limit $Q^2 \to 0$, i.e.

$$\sigma_D^L = \frac{4\pi^2\alpha}{v}\left[\frac{v^2}{Q^2} W_{2D} - W_{1D}\right] \xrightarrow[Q^2\to 0]{} 0. \tag{42}$$

In the light front approach this condition is satisfied as follows. The physical nucleon structure functions treated as functions of q^2 and W^2 satisfy the analogous constraint

$$\frac{\nu_p^2}{Q^2} W_{2p} - W_{1p} \xrightarrow[Q^2\to 0]{} 0, \tag{43}$$

where

$$\nu_p = \frac{pq}{m} = \frac{Wq+Q^2}{m}. \tag{44}$$

From Eqs. (40) and (43) it follows that for $Q^2 \to 0$

$$\sigma_D^L = \frac{4\pi^2\alpha}{\nu} \sum_{p=\text{proton}}^{\text{neutron}} \int d^3kf(\vec{k}) \frac{m}{p^+} \left[\frac{\nu^2 p^{+2}}{(Wq)^2} - 1 \right] W_{1p}. \tag{45}$$

In contrast to the conventional approaches we have always $q^+ = 0$. Therefore,

$$Wq \xrightarrow[q^+ \to 0]{} \tfrac{1}{2} p^+ q^- = p^+ \nu \tag{46}$$

and the condition Eq. (42) is satisfied without invoking ad hoc corrections. In other words, we have satisfied the identity

$$\tilde{p}q \equiv pq \tag{47}$$

giving $\nu_{\tilde{p}} \equiv \nu_p$, and being once more the manifestation of the fact that the light front dynamics is developed on the properly chosen zero hyperplane, as was explained in Sec. 2.

C. Moments and sum rules

In the Bjorken limit Eqs. (40) give scaling structure functions

$$F_{1D} = 2MW_{1D} = \sum_{p=\text{proton}}^{\text{neutron}} \int d^3kf(\vec{k}) \frac{1}{y} F_{1p}\left(\tilde{p}^2, \frac{x}{y}\right),$$

$$F_{2D} = \nu W_{2D} = \sum_{p=\text{proton}}^{\text{neutron}} \int d^3kf(\vec{k}) F_{2p}\left(\tilde{p}^2, \frac{x}{y}\right), \tag{48}$$

where

$$y = \frac{p^+}{D^+} = \tfrac{1}{2}\left(1 + \frac{k^3}{\sqrt{m^2 + \vec{k}^2}}\right) \tag{49}$$

and from Sec. 4 we have

$$F_{2p}(\tilde{p}^2, z) = N(\tilde{p}^2) z^\alpha \left(\mu^2 + \frac{m_c^2}{1-z} - \tilde{p}^2\right)^{-3},$$

$$F_{1p} = \frac{1}{z} F_{2p}. \tag{50}$$

The threshold condition $\theta(y-x)$ matching with the conservation of the positive value of the plus component of the total momentum, is implicitly included.

The moments of the deuteron structure functions

$$M_n^D = \int_0^1 dx x^n F_{2D}(x) \tag{51}$$

are calculated by inverting relations Eq. (49) or Eq. (13)

$$\vec{k}^2 = \frac{\vec{k}^{\perp 2} + 4(y-\frac{1}{2})^2 m^2}{4y(1-y)} . \tag{52}$$

Changing the order of the integration over x and y in Eq. (51) we get

$$M_n^{\mathrm{D}} = \sum_{\mathrm{p=proton}}^{\mathrm{neutron}} \int d^3k f(\vec{k}) y^{n+1} \int_0^1 dz z^n F_{2\mathrm{p}}(\tilde{p}^2, z) \tag{53}$$

where

$$\tilde{p}^2 = (D-n)^2 = m^2 - 4y(m\varepsilon + \vec{k}^2), \tag{54}$$

and it depends on y and $\vec{k}^{\perp 2}$. Without this dependence the n-th deuteron moment M_n^{D} would be the following product

$$M_n^{\mathrm{D}} = M_{n+1}^{\mathrm{f}} \cdot (M_n^{\mathrm{P}} + M_n^{\mathrm{N}}). \tag{55}$$

The off-shell effects complicate the product form in Eq. (55) into the convolution in Eq. (53).

For $n = -1$ it follows that

$$\int_0^1 dx \frac{F_{2\mathrm{D}}(x)}{x} = \sum_{\mathrm{p=proton}}^{\mathrm{neutron}} \int_0^1 dz \frac{F_{2\mathrm{p}}(\tilde{p}^2, z)}{z} , \tag{56}$$

where, in fact, the r.h.s. of Eq. (56) is independent of $\tilde{p}^2$, thanks to the sum rule in Eq. (31). Thus, we are led to the parton-like picture with the satisfied charge sum rule, even if we include the dynamical off-shell corrections. The light front approach resolves the contradiction with the parton model expectations encountered in the conventional approaches (see Sec. 6).

D. Deuteron Fermi smearing corrections

To show the size of the Fermi smearing effects in deuteron we assume that the nucleon structure function $F_2(\tilde{p}^2, z)$ in Eq. (48) is independent of $\tilde{p}^2$. Then Eq. (48) gives the following smearing expression

$$F_{2\mathrm{D}}(x) = \int_x^1 dy \varrho(y) \left[F_{2\mathrm{P}}\left(\frac{x}{y}\right) + F_{2N}\left(\frac{x}{y}\right) \right], \tag{57}$$

where $\varrho(y) = M \int d^2k^{\perp} f(\vec{k})$. For example, the Hulthen-Sugawara wave function [15]

$$\phi_0 \sim (m\varepsilon + \vec{k}^2)^{-1} (\lambda^2 + \vec{k}^2)^{-1}, \quad \lambda^2 \cong 0.05\ \mathrm{GeV}^2 \tag{58}$$

gives

$$\varrho(y) = A[(m\varepsilon+\delta^2)^{-1} + (\lambda^2+\delta^2)^{-1} - 2(\lambda^2 - m\varepsilon)^{-1} \ln (\lambda^2+\delta^2)(m\varepsilon+\delta^2)^{-1}], \tag{59}$$

where $\delta^2 = m^2(y-\frac{1}{2})^2 y^{-1}(1-y)^{-1}$, and the normalization constant A is given by

$$\int_0^1 \varrho(y)dy = 1, \tag{60}$$

following from Eq. (19). The momentum sum rule is

$$\langle (y-\tfrac{1}{2})\rangle_\varrho = \int_0^1 \varrho(y)\,(y-\tfrac{1}{2})dy = 0. \tag{61}$$

The size of the Fermi smearing effects is shown in Fig. 11. One defines the smeared structure function

$$F_\varrho(x) = \int_x^1 \varrho(y) F\left(\frac{x}{2y}\right), \tag{62}$$

which corresponds to the structure function $F_D\left(\frac{x}{2}\right)$. This rescaling by factor 2 is implicitly introduced in the following considerations. The smearing ratio $R(x)$ is

$$R(x) = \frac{F(x)}{F_\varrho(x)}. \tag{63}$$

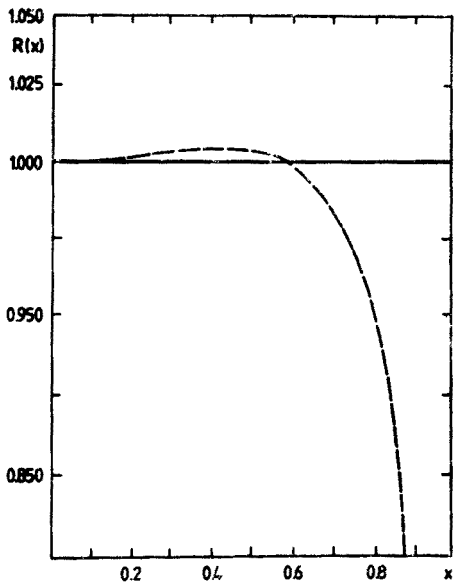

Fig. 11. The deuteron smearing ratio $R(x)$ from Eq. (63), for the example of the proton structure function $F_2(x)$ from Ref. [14], for $Q^2 = 10\,\mathrm{GeV}^2$, and the soft core Hulthen-Sugawara deuteron wave function from Ref. [15]

The shape of $R(x)$ depends mainly on the nucleon structure itself, and is practically independent of the detailed behaviour of the density $\varrho(y)$. Because $\varrho(y)$ is sharply peaked around $y = \frac{1}{2}$, the following formula

$$F_\varrho = F + \tfrac{1}{2} \cdot (x^2F')' \cdot \langle (2y-1)^2 \rangle_\varrho \tag{64}$$

describes the shape of $R(x)$ including the rapid variations of $R(x)$ for $x > 0.6$. The ratio of $(x^2F'_{2P})'$ to F_{2P} rises to infinity when x approaches 1. However, for $x \lesssim 0.6$ it is of the order of -2, while $\langle (2y-1)^2 \rangle_\varrho$ for the deuteron is equal to about 0.4%. Therefore the properly calculated Fermi smearing for $x < 0.6$ amounts to the following relation

$$F_{2D} = F_{2P} + F_{2N} \tag{65}$$

which is of accuracy much better than 1%. The relation Eq. (65) is exact for $x = 0$ and at $x = x_0$, where $x_0 \sim 0.6$, it is the zero point of the function $[x^2(F'_{2P} + F'_{2N})]'$. The validity of Eq. (65) at x_0 is a consequence of the sharp peaking of $\varrho(y)$, around $y = \frac{1}{2}$, corresponding to $x = 1$, see Eq. (62). The expansion Eq. (64) is very useful in the analysis of the EMC effect [16].

E. Dynamical effects

The dynamical effects in our model calculation follow from the $\tilde{p}^2$-dependence of the nucleon structure functions. From Eq. (50) we get

$$F_{2p}(\tilde{p}^2, z) = N(m^2 - d^2) z^\alpha \left(\mu^2 + \frac{m_c^2}{1-z} - m^2 + d^2 \right)^{-3}, \tag{66}$$

where

$$d^2 = m^2 - \tilde{p}^2 = 4y(m\varepsilon + \vec{k}^2). \tag{67}$$

For a free nucleon the value of d^2 is equal to zero.

The dynamical change of the shape of a bound nucleon structure function arises as follows. The positive correction d^2 enlarges the denominator in Eq. (66), and it diminishes F_2 as it is shown in Fig. 12. There is no change of the shape in the perturbative region,

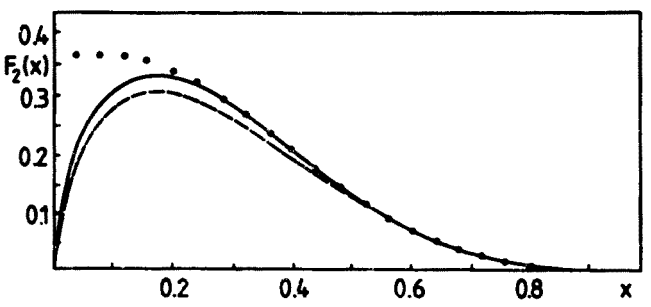

Fig. 12. The dynamical change of the bound nucleon structure function in the deuteron, caused by the presence of d^2 in Eq. (66), and compared with the fit to the proton structure function F_{2p} at $Q^2 = 15$ GeV^2, from Ref. [14]. The full line is for the free, and the broken line for the bound nucleon

where $z \to 1$, and the value of the d^2 correction is negligible in comparison with $m_c^2(1-z)^{-1}$. The normalization constant $N(m^2-d^2)$ has to become larger than $N(m^2)$, to preserve the sum rule Eq. (31), following from the charge conservation law. Effectively, the structure function $F_2(\tilde{p}^2, z)$ is smaller than $F_2(m^2, z)$ for small z, and larger than $F_2(m^2, z)$ for large z. Their ratio at $z = 1$ is equal to the ratio $N(m^2-d^2)/N(m^2)$.

Finally, using result Eq. (65), we can write

$$F_{2D}(x) = F_{2P}(\langle\tilde{p}^2\rangle_D, x) + F_{2N}(\langle\tilde{p}^2\rangle_D, x). \tag{68}$$

The ratio of the proton structure function $F_{2P}(\langle\tilde{p}^2\rangle_D, x)$ to the free proton structure function $F_{2P}(m^2, x)$ is plotted in Fig. 13. The size of dynamical effect depends on para-

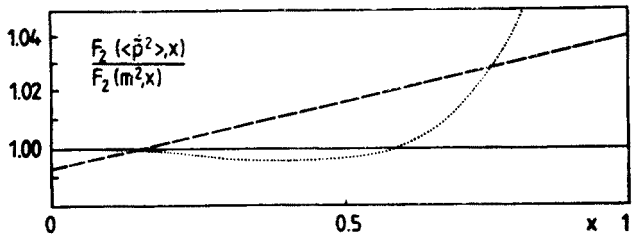

Fig. 13. The ratio of the averaged virtual proton structure function $F_2(\langle\tilde{p}^2\rangle_D, x)$ to the free proton structure function $F_2(m^2, x)$, after imposing the charge conservation constraint. It is shown by the dashed line. The dotted line represents the Fermi smearing effect

meters μ^2, m_c^2, and α in Eq. (66). Note that the x-dependence of the denominator in Eq. (66) is governed only by the ratio $s = (m^2-\mu^2)/m_c^2$, which was found to be equal to 0.097 in Sec. 4, in order to reproduce the experimental behaviour of the proton structure function F_{2P}, see Fig. 9. The corresponding value $\alpha = 0.67$ is close to the expected value 0.5 [11]. Therefore, the size of the dynamical effects directly depends on the ratio of

$$m^2 - \langle\tilde{p}^2\rangle_D = \langle d^2\rangle_D \sim 2\langle\vec{k}^2\rangle_D \sim 0.02\, m^2 \tag{69}$$

to the core mass m_c^2. In Fig. 13 we took $m_c = 0.85$ GeV, assuming that it lies between two constituent quark masses, and the nucleon mass.

The above example shows that the dynamical effects are bigger than the smearing corrections for $x < 0.6$. From Eq. (64) we see that the smearing corrections are of the order of $\frac{1}{3}\left\langle\frac{\vec{k}^2}{m^2}\right\rangle_D$, i.e. 0.5%, while from Eq. (68) we get the dynamical correction of the order of $3\left\langle\frac{d^2}{m_c^2}\right\rangle_D = 2\cdot 3\cdot\left\langle\frac{\vec{k}^2}{m_c^2}\right\rangle_D$, corrected by the sum rule. The factor 3 comes from the power -3 in Eq. (66), implied by counting rules, and the factor 2 from the number of nucleons $4\langle y\rangle_D = 2$ in Eq. (67). If we allow an off-shell continuation of the bound nucleon structure, varying only G_0 in the nucleon wave function $\Psi = G_0\phi$, without alteration of the vertex function ϕ, then the factor 3 is replaced by 2. Therefore, our conclusion about the size of the dynamical effects is more general than the tree diagram model used in the present calculation.

F. Extracting neutron structure

The neutron structure functions can be extracted from the deuteron and the proton data using Eq. (40). In the Bjorken limit one can use Eq. (57) including a Q^2-dependence of the structure functions, and also the extremely simple Eq. (64) for $x \lesssim 0.6$. Considering that 0.5% accuracy is sufficient and ignoring the dynamical effects, one can write, from Eq. (65)

$$F_{2N} = F_{2D} - F_{2P} \tag{70}$$

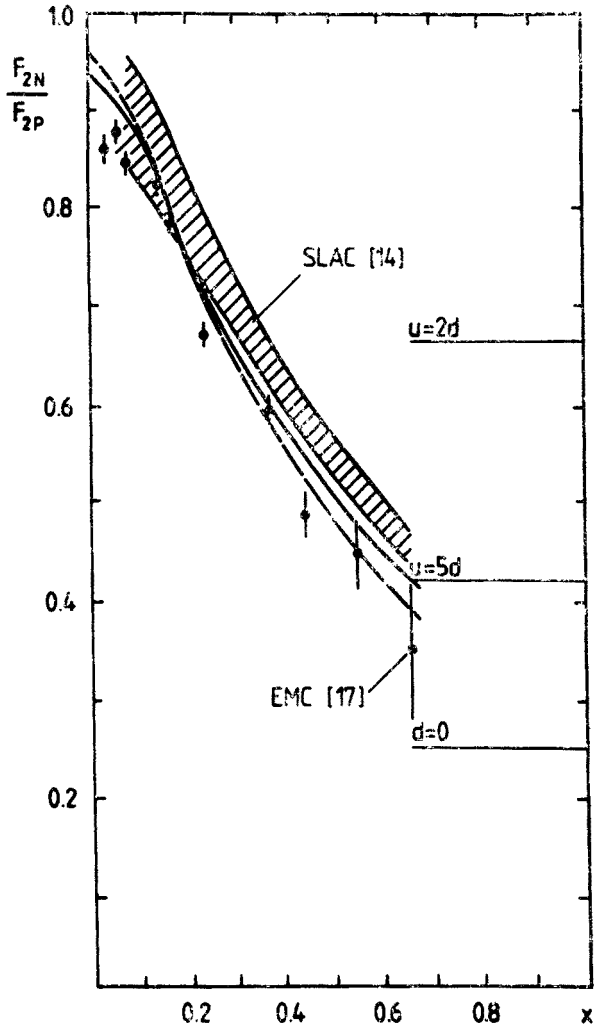

Fig. 14. The ratio of the neutron to the proton structure functions extracted from the deuteron and the proton data from Ref. [14]. The full line is obtained by neglecting the dynamical effects, and the dashed one by including them

for $x < 0.6$. However, the dynamical effects cannot be neglected, as it is shown in Sec. 5.E. Our model calculation of these effects, assumed to be equal for both nucleons in order to avoid complicated discussion, results in the modified equation

$$F_{2N} = F_{2D}(1+0.05(x-0.15))^{-1} - F_{2P}, \tag{71}$$

where we put the smearing ratio $R(x) = 1$, and used a linear fit to the dashed line from Fig. 13. The influence of the dynamical correction on the extracted ratio F_{2N}/F_{2P} is shown in Fig. 14. For example, the extracted d/u ratio at $x \sim 0.6$, including the dynamical effects is 20% smaller than the same ratio extracted without the dynamical corrections.

6. Comparison with other approaches

The first detailed consideration of the deuteron smearing corrections in the electron-deuteron scattering was published by West [18] in 1972. Since that time a number of authors treated this subject [14, 18–22], trying to solve problems of the two nucleon approximation. All of them, in fact, start from Eq. (1), but none of them specifies the conditions, which would justify the factorization of $W_D^{\mu\nu}$ represented by the diagram of Fig. 1 into the form of Eq. (1). How does this factorization emerge in the light front approach is explained in Sec. 5.A. The problem of the identification of the density $\varrho(p)$ in Eq. (1) was not clarified and once more it was stressed in the last paper of Kusno and Moravcsik (1983). Frankfurt and Strikman [20] identify $\varrho(p)$ with the nonrelativistic wave function via the Weinberg wave function but inconsistently remove the factor $\sqrt{m^2+\vec{k}^2}$ from the normalization condition, forcing its presence in the Weinberg wave function. This was shown in Sec. 3 to contradict the connection between the Weinberg and the Schrödinger equation. It can be treated only as a phenomenological device dictated by the lack of a complete light front description of the nucleon-nucleon interaction.

In contrast to other approaches [14, 18–22] starting from Eq. (1), we consider the Compton scattering amplitude on the active quark in Figs. 8 and 10 as an elementary amplitude, undergoing the smearing in the electron-nucleon, or in the electron-deuteron scattering. This insight into the quark structure of the nucleons results in the full control of the off-shell effects, in a simple model calculation, with more general, model-independent consequences. Namely, we provide the identification of the off-shell nucleon structure functions with the on-shell ones, preserving the proper threshold behaviour, which solves the Bodek problem [19] ($\sigma_D^L \not\to 0$, when $Q^2 \to 0$), without ad hoc artificial corrections. This is explained in Sec. 2 and 5.B. The origin of this success lies in the proper choice of the light front direction which gives exactly $q^+ = 0$. None of the methods [14, 18–22] provides such a universal prescription.

West introduced the so called West-β correction [18], later on argued to be zero by Frankfurt and Strikman [20], and Landshoff and Polkinghorn [21], and recently discussed by Kusno and Moravcsik [22] in different aspects. The light front approach confirms the statement that the West-β correction is not present [20, 21, 22], as it is explained in Sec. 5.D. The condition $q^+ = 0$ removes the limits, imposed on the phase space of the spectator

nucleon in the West-Atwood approach [18, 14], leading to the β correction. At the same time the light front method leads directly to the parton model expectations which were questioned by Kusno and Moravcsik in 1983.

The model calculations of the dynamical effects, and their influence on the extracted neutron structure function have not been considered yet, in the previous papers.

7. *Summary and conclusions*

Thus far, the extensive efforts in describing the deep inelastic structure of the deuteron have been carried out in the two nucleon approximation. Different aspects of the deuteron binding effects were considered, but inherent problems of the two nucleon approximation, having influence on data analysis, have not been consistently solved.

As we have described in this paper, the detailed model calculations of the diagram from Fig. 10 in the light front scheme provide an example of the conventional two nucleon approximation free from the problems encountered in other approaches. The basic quantity to be considered is the virtual Compton scattering on quarks, belonging to the struck nucleon. A particular structure of the nucleon-quark vertex in Fig. 10 leads to the smearing expression ($\mu, \nu = +, \perp$)

$$W_D^{\mu\nu} = \int d^3p\varrho(p)\,(W_P^{\mu\nu} + W_N^{\mu\nu}).$$

The density $\varrho(p)$ is related to the two nucleon Fock wave function on the light front. To solve the specific problems of the two nucleon approximation one has to choose a special light front direction. The experimental conditions select the z axis in the laboratory frame, which deviates from the momentum transfer $\vec{q}$, carried by the photon, by an angle α, where $\operatorname{tg}\alpha = \frac{Q}{\nu}$. Just this subtle deviation is the origin of the success of the light front approach. It yields always the condition $q^+ = 0$, and the relevant structure functions can be expressed by the appropriate Fock components in a simple manner intuitively expected from non-relativistic quantum mechanics. The two nucleon light front wave function is shown to be exactly equal to the nonrelativistic deuteron wave function, outside the range of a potential. However, the relativistic Fock wave function is normalized including a factor $\sqrt{m^2+\vec{k}^2}$, where $\vec{k}$ is the relative momentum of nucleons in their center of mass frame of reference.

The off-shell continuation of the bound nucleon structure functions according to the light front rules does not violate the condition $\sigma_D^L \to 0$ for $Q^2 \to 0$, preserving the proper threshold behaviour.

In the Bjorken limit we reproduce the parton model formulae, with the satisfied sum rules. The smearing corrections to the additivity relation for the structure functions

$$F_{2D} = F_{2P} + F_{2N}$$

are at most equal to 0.5%, up to $x \lesssim 0.6$. The additivity is exact at $x = 0$. The so called β correction is absent.

The model calculation of the dynamical off-shell effects in the deep inelastic structure functions of bound nucleons shows that the effects are several times larger than the smearing corrections. They lower the extracted neutron structure function at large x, and bring it closer to the parton model limit of 0.25. The inclusion of these effects gives the extracted d/u ratio in proton at $x \sim 0.6$ diminished by 20%.

The light front methods discussed in this paper and illustrated for the two nucleon sector are equally applicable to other components of the deuteron.

The author would like to thank Professor J. M. Namysłowski for stimulating concern extended to him at the Warsaw University where this work was done.

APPENDIX

Details of calculating the structure function

From Eq. (27) we get in Eq. (26) the following result

$$\frac{1}{2}\sum_{s_p s_a'} j_p^{\mu *} j_p^{\nu} = \frac{1}{2}|\psi_p(a)|^2 \frac{1}{4p^+ a^+} \operatorname{Tr} \not{n}(\not{a}+m_a)\gamma^{\mu}(\not{a}'+m_a)\gamma^{\nu}(\not{a}+m_a)\not{n}(\not{p}+m). \tag{A.1}$$

The trace part can be written as

$$4p^+ a^+ \operatorname{Tr}(\not{a}+m_a)\gamma^{\mu}(\not{a}'+m_a)\not{n}\gamma^{\nu} \tag{A.2}$$

Now we use a trick

$$a' = a+q+\sigma, \quad \sigma = \tfrac{1}{2}\sigma^- \eta, \quad \sigma^- = a'^- - a^- - q^- \tag{A.3}$$

and note, that $q^+ = 0$ implies

$$(q+\sigma)^2 = q^2. \tag{A.4}$$

The trace in Eq. (A.2) is

$$2q^2\left(g^{\mu\nu} - \frac{(q+\sigma)^{\mu}(q+\sigma)^{\nu}}{q^2}\right) + 8\left(a^{\mu} - \frac{a(q+\sigma)}{q^2}q^{\mu}\right)\left(a^{\nu} - \frac{a(q+\sigma)}{q^2}q^{\nu}\right). \tag{A.5}$$

Subtracting a longitudinal part [10], $j^{\nu} \to j^{\nu} - \dfrac{jq}{q^2}q^{\nu}$, or

$$W^{\mu\nu} \to (W^{\mu\beta} - q^{\mu}q_{\alpha}W^{\alpha\beta}/q^2)\left(\delta_{\beta}^{\nu} - \frac{q_{\beta}q^{\nu}}{q^2}\right),$$

we get

$$2q^2\left(g^{\mu\nu} - \frac{q^{\mu}q^{\nu}}{q^2} - \frac{\sigma^{\mu}\sigma^{\nu}}{q^2}\right) + 8\left(a^{\mu} - \frac{aq}{q^2}q^{\mu}\right)\left(a^{\nu} - \frac{aq}{q^2}q^{\nu}\right). \tag{A.6}$$

Then follows Eq. (27) with W_1 and W_2 given in Eq. (28). Similar calculation leads from Eq. (36) to Eq. (40).

REFERENCES

[1] T. E. O. Ericson, *The Deuteron Properties*, Invited talk at: Few Body X, 10th International Conference on Few Body Problems in Physics, Karlsruhe, Germany, August 21–27, 1983; Ref. TH 3719-CERN, September 1983.

[2] J. M. Namysłowski, *J. Progr. Part. Nucl. Phys.* **14**, 1 (1984). This paper contains an extensive review of the light front techniques, with applications.

[3] G. P. Lepage, S. J. Brodsky, *Phys. Rev.* **D22**, 2157 (1980); G. P. Lepage, S. J. Brodsky, T. Huang, P. B. Mackenzie, Banff Summer Institute on Particle Physics, Banff, Alberta, Canada, August 1981, also CLNS-82/522; S. J. Brodsky, G. P. Lepage, (SLAC-PUB-2447) 1979 Summer Institute on Particle Physics at SLAC, Stanford, California; S. J. Brodsky, G. P. Lepage, *Phys. Scr.* **23**, 945 (1981); S. J. Brodsky, T. Huang, G. P. Lepage, (SLAC-PUB-2868), Proceedings of the KfK Summer School on Quarks and Nuclear Forces (1981), *Quarks and Nuclear Forces*, ed. D. Fries and B. Zeitnitz, Springfield 1982.

[4] S. J. Brodsky, S. D. Drell, *Phys. Rev.* **D22**, 2236 (1980); St. Głazek, J. M. Namysłowski, in preparation.

[5] S. Weinberg, *Phys. Rev.* **150**, 1313 (1966).

[6] St. Głazek, *Acta Phys. Pol.* **B15**, 889 (1984).

[7] H. Leutwyler, J. Stern, *Ann. Phys.* (N.Y.) **112**, 94 (1978). In calculations based on field theory (like QCD) one can bypass this problem evaluating invariant quantities, see Ref. [2] for further discussion.

[8] F. Gross, *Phys. Rev.* **140**, B410 (1965).

[9] S. J. Brodsky, R. Roskies, R. Suaya, *Phys. Rev.* **D8**, 4574 (1973).

[10] R. P. Feynman, *Photon-Hadron Interaction*, North-Holland/American Elsevier 1976.

[11] J. F. Gunion, S. J. Brodsky, R. Blankenbecler, *Phys. Rev.* **D8**, 287 (1973); S. J. Brodsky, F. E. Close, J. F. Gunion, *Phys. Rev.* **D8**, 3678 (1973); M. Chemtob, *Nuovo Cimento* **71A**, 447 (1982).

[12] A. Głazek et al., *Phys. Lett.* **158B**, 150 (1985).

[13] R. C. Hwa, *Phys. Rev.* **D22**, 759 (1980).

[14] A. Bodek et al., *Phys. Rev.* **D20**, 1471 (1979).

[15] L. Hulthen, M. Sugawara, *Encyclopedia of Physics* **39**, Springer 1957, p. 92.

[16] St. Głazek, M. Schaden, *Z. Phys.* **A323**, 451 (1986).

[17] K. Rith, in Proceedings of the International Europhysics Conference on High Energy Physics, Brighton, July 1983, ed. J. Guy and C. Costain, Rutherford Appleton Laboratory, Chilton, Didcot, UK; p. 80.

[18] G. B. West, *Ann. Phys.* (N.Y.) **74**, 464 (1972); W. B. Atwood, G. B. West, *Phys. Rev.* **D7**, 773 (1973).

[19] A. Bodek, *Phys. Rev.* **D8**, 2331 (1973).

[20] L. L. Frankfurt, M. I. Strikman, *Phys. Lett.* **64B**, 433 (1976); *Phys. Lett.* **65B**, 51 (1976); *Phys. Lett.* **76B**, 333 (1978); *Nucl. Phys.* **B148**, 107 (1979); *Phys. Rep.* **C76**, 215 (1981).

[21] P. V. Landshoff, J. C. Polkinghorn, *Phys. Rev.* **D18**, 158 (1978).

[22] D. Kusno, M. J. Moravcsik, *Phys. Rev.* **D20**, 2734 (1979); *Nucl. Phys.* **B184**, 283 (1981); D. Kusno, *Phys. Rev.* **D26**, 3276 (1982); D. Kusno, M. J. Moravcsik, *Phys. Rev.* **C27**, 2173 (1983).